

Average resonance capture studies of $^{162,164}\text{Dy}$

D. D. Warner, R. F. Casten, and W. R. Kane
Brookhaven National Laboratory, Upton, New York 11973

W. Gelletly

Schuster Laboratory, University of Manchester, Manchester M13 9PL, United Kingdom

(Received 22 December 1982)

Primary γ -ray transitions in ^{162}Dy and ^{164}Dy have been studied following average resonance neutron capture with neutron beams of mean energy 2 and 24 keV. The averaging process guarantees the observation of the complete set of $J^\pi = 1^{-(+)}, 2^\pm, 3^\pm, 4^{-(+)}$ states in ^{162}Dy (^{164}Dy) up to an excitation energy of 2 MeV. Use of the results of recent Monte Carlo calculations has been made to establish semiquantitative criteria for the J^π assignments. Further spin limitations have been imposed by the study of primary transitions following capture in the 2.72 and 3.68 eV resonances in ^{162}Dy and the 1.71 eV resonance in ^{164}Dy . The known completeness of the set of observed levels has been used to establish a correspondingly complete band structure in both nuclei. The results are discussed in the framework of both the interacting boson approximation and the geometrical model.

NUCLEAR REACTIONS $^{161,163}\text{Dy}(n,\gamma)$, $E_n = \text{res}, 2 \text{ keV}, 24 \text{ keV}$; measured E_γ, I_γ ; $^{162,164}\text{Dy}$ deduced levels, J, π , band structure. Ge(Li) detectors, enriched targets, ARC spectroscopy. Comparison with predictions of interacting boson approximation and geometrical model.

I. INTRODUCTION

The region of well deformed nuclei might well be considered one of the best understood in terms of nuclear structure. However, the recent application¹ of the interacting boson approximation² (IBA) to this class of nuclei has resulted in the prediction of a number of new features which are in many cases at variance with the expectations of the simple geometrical model. As an example, the predicted characteristics³ of the lowest excited $K^\pi = 0^+$ band differ substantially in the two approaches but, unfortunately, the identification and dominant decay modes of such excitations are, in general, poorly established. There is also little detailed experimental information available with which to test the predictions of the two models concerning the predicted two phonon excitations built on the β and γ modes. In the case of negative parity (octupole) excitations, while a large number of negative parity bands with collective character were identified throughout the deformed region, it is necessary to identify the complete set of predicted excitations ($K^\pi = 0^- - 3^-$) across the region, and their dominant decay modes, in order to obtain an understanding of the general

characteristics of such excitations and allow a comparison with model predictions.

In general, therefore, one prerequisite for an improved understanding of deformed nuclei is the establishment of complete sets of collective excitations below the pairing gap in a number of nuclei. The (n,γ) reaction is ideal for such a purpose, since it can populate low spin states of widely differing structure. Indeed, the technique of average resonance capture (ARC) can provide, in appropriate cases, a guarantee that all states within a certain range of J^π values and excitation energy will be populated. The consequences and implications of such a guarantee have been discussed in general terms in a previous publication,⁴ the most striking specific example of the use of the ARC technique being the study of ^{168}Er ,⁵ where the identification of the complete set of low K bands below the pairing gap allowed an unambiguous comparison to be made with the predictions of the IBA formalism.¹ The current study was therefore undertaken to establish similarly complete sets of low spin states, and hence the low K band structure, in the nuclei ^{162}Dy and ^{164}Dy via measurements of the primary γ -ray spectra resulting from $^{161}\text{Dy}(n,\gamma)^{162}\text{Dy}$ and $^{163}\text{Dy}(n,\gamma)^{164}\text{Dy}$ ARC spectroscopy.

II. EXPERIMENTAL TECHNIQUE

Primary γ -ray spectra were studied following neutron capture in targets of ^{161}Dy and ^{163}Dy , with mean neutron energies of 2 and 24 keV in each case, using the tailored beam facility at the high flux beam reactor of Brookhaven National Laboratory. Filters of Sc and ^{56}Fe were used to provide neutron beams centered at 2 and 24 keV, respectively, the corresponding effective FWHM being ≈ 0.85 and ≈ 1.9 keV. The primary γ -ray spectra were recorded with a three crystal pair spectrometer. A detailed description of this facility has been given elsewhere.⁶

The two targets for these measurements consisted of 33.8 and 34.4 g of dysprosium oxide enriched to 95.94% and 92.98% in ^{161}Dy and ^{163}Dy , respectively. The γ -ray spectra were recorded in a 8192 channel ADC and the system was stabilized against zero and gain drift with a high precision dual pulser. Energy and efficiency calibrations were obtained in each case from an accompanying thermal capture measurement with a 1 g target of NaCl, the calibration energies and intensities being taken from the work of Stelts and Chrien.⁷ While the majority of contaminants observed in the current measurement could be identified from the results of earlier stud-

ies, it was also possible to distinguish contaminants from average capture lines by using the fact that the former usually arise following the capture of ambient thermal neutrons, and thus lead to lines of identical energies in the 2 and 24 keV spectra, whereas a line representing a transition to a given final state will occur 22 keV higher in energy for $E_n=24$ keV than for $E_n=2$ keV. This feature is evident in Fig. 1, which shows the 2 and 24 keV spectra of ^{164}Dy . The 24 keV spectrum has been displaced by 22 keV relative to the 2 keV spectrum, so that peaks corresponding to levels in ^{164}Dy are aligned in the two spectra, while contaminants are not. As an example, the doublet occurring at the far right arises from thermal capture in Fe and, as can be seen, it appears at different positions in the two spectra.

In addition to the ARC measurements, Ge(Li) singles measurements were also made of the primary spectra following single resonance capture in the two target nuclei using the neutron monochromator facility⁸ at BNL. Specifically, the 1.713 eV (2^-) resonance in ^{164}Dy and the 2.72 eV (3^+) and 3.68 eV (2^+) resonances in ^{162}Dy were studied.

III. RESULTS

The ARC technique greatly reduces the statistical fluctuations in primary intensities that would arise in single resonance, or thermal, neutron capture. This is the result of the spread in energy of these neutron beams, which encompasses a large number of individual resonances. Clearly, therefore, the extent to which these fluctuations are reduced will depend on the number of resonances in the neutron energy interval, and thus on the level density for certain J^π values above the binding energy of the target nucleus. To interpret the data, it is convenient to remove the secular energy dependence of the primary intensities by defining "reduced" intensities as I_γ/E_γ^n , where n has been determined empirically as 5. The fluctuation in the reduced intensities is then given approximately by $2/\sqrt{N}$, where N is the number of resonances in the effective averaging interval.

Thus, given a sufficient number of resonances in the averaging interval, the ARC technique provides two powerful capabilities. Firstly, since the population intensity of a given final state depends only on its J^π value, and not on its structure, states of the same J^π values will be populated with approximately equal reduced intensity, and thus the measured intensities yield substantial J^π information. Perhaps more importantly, *all* states of a given J^π value *must* be populated, up to an excitation energy determined by the E_γ^5 factor and the sensitivity of the measurement. The range of J^π values for which a complete

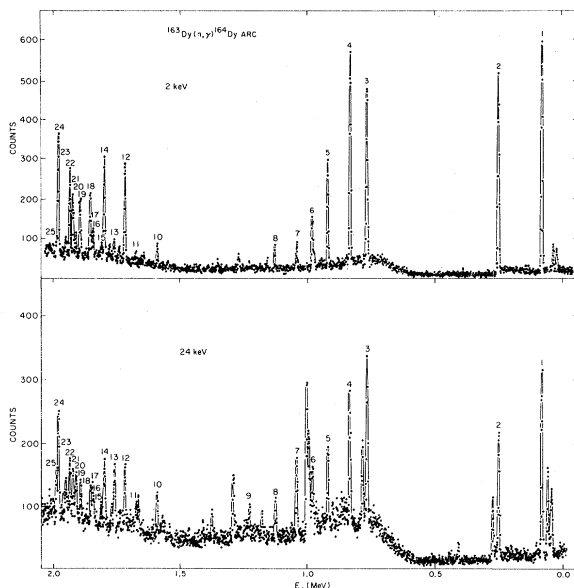


FIG. 1. Primary γ -ray spectra observed in 2 and 24 keV neutron capture into ^{164}Dy . The abscissa corresponds to excitation energy in ^{164}Dy . Peaks corresponding to transitions in ^{164}Dy are numbered; other peaks are contaminants.

TABLE I. High Energy γ rays in ^{162}Dy observed in 2 and 24 keV capture. Errors on the last digit of the energies and intensities are given in parentheses.

E_x (keV)	2 keV		24 keV		$\frac{I_R(2\text{ keV})}{I_R(24\text{ keV})}$	J^π ^b
	E_γ (ΔE_γ) (keV)	$(I_\gamma/E_\gamma^5)^a$ (keV)	E_γ (ΔE_γ) (keV)	$(I_\gamma/E_\gamma^5)^a$ (keV)		
80.6(3)	8118.2(3)	100(4)	8140.1(3)	100(4)	1.00(6)	2 ⁺ , 3 ⁺
265.5(4)	7933.3(3)	61(3)	7955.6(4)	73(4)	0.84(6)	4 ⁺
888.6(4)	7310.2(3)	99(5)	7332.6(4)	106(6)	0.94(7)	2 ⁺ , 3 ⁺
962.8(4)	7236.0(4)	94(5)	7257.9(4)	116(6)	0.81(6)	2 ⁺ , 3 ⁺
1060.7(4)	7138.0(4)	71(5)	7160.0(4)	80(6)	0.89(9)	4 ⁺ (2 ⁺)
1148.3(3)	7050.5(3)	636(13)	7072.7(3)	220(9)	2.89(14)	2 ⁻ , 3 ⁻
1210.2(3)	6988.6(3)	592(13)	7010.8(3)	218(9)	2.72(13)	2 ⁻ , 3 ⁻
1275.8(3)	6923.0(3)	337(12)	6945.1(4)	106(8)	3.20(27)	1 ^{-c}
1297.1(3)	6901.7(3)	392(12)	6923.9(4)	154(9)	2.54(17)	4 ⁻
1358.0(3)	6840.8(3)	655(15)	6862.9(3)	222(11)	2.95(16)	2 ⁻ , 3 ⁻
1453.8(5)	6745.0(4)	98(8)	6767.6(6)	76(11)	1.29(21)	2 ⁺ (3 ⁺ , 4 ⁺)
1535.8(7)	6663.0(7)	46(10)	d			1 ⁺ , 4 ⁺ (2 ⁺ , 3 ⁺)
1571.0(3)	6627.8(3)	629(17)	6649.7(5)	258(27)	2.44(26)	2 ⁻ , 3 ⁻
1575.6(13)	6621.6(12)	53(11)	6645.3(13)	63(24)	0.84(36)	1 ⁺ , 4 ⁺ (2 ⁺ , 3 ⁺)
1637.2(3)	6561.6(3)	317(13)	6584.5(5)	94(11)	3.36(41)	1 ⁻ (4 ⁻)
1669.0(3)	6529.8(3)	369(14)	6552.1(4)	156(12)	2.37(21)	4 ⁻
1691.4(3)	6507.4(3)	692(19)	6529.9(4)	228(15)	3.04(21)	2 ⁻ , 3 ⁻
1728.2(5)	6470.6(4)	131(12)	6492.0(5)	109(14)	1.20(19)	2 ⁺ , 3 ⁺
1739.1(3)	6459.7(3)	514(18)	6482.3(4)	248(16)	2.08(15)	2 ⁻ , 3 ⁻
1746.2(9)	6452.6(9)	32(16) ^e	6475.0(7)	79(13)	0.41(21) ^e	4 ⁺ (1 ⁺)
1766.5(3)	6432.3(3)	674(20)	6454.8(4)	306(24)	2.21(19)	2 ⁻ , 3 ^{-f}
1782.2(5)	6416.6(5)	107(12)	6439.7(7)	114(26)	0.94(24)	2 ⁺ , 3 ⁺ (4 ⁺)
1826.6(4)	6372.2(3)	308(17)	d			4 ^{-f}
1840.3(5)	6358.5(5)	109(15)	6381.0(6)	69(26) ^e	1.58(63)	2 ⁺ , 3 ⁺ (4 ⁺)
1851.9(4)	6346.9(3)	342(22)	6369.3(5)	159(18)	2.15(28)	4 ^{-g}
1863.6(3)	6335.2(3)	1055(24)	6357.9(5)	317(39)	3.33(42)	2 ⁻ , 3 ^{-h}
1887.1(6)	6311.7(5)	108(33) ^e	6334.4(6)	94(15)	1.15(35)	2 ⁺ , 3 ⁺ , 4 ⁺
1895.2(5)	6303.6(5)	131(14)	6325.6(7)	89(18)	1.47(34)	2 ⁺ , 3 ⁺
1910.7(3)	6288.1(3)	679(20)	6309.4(4)	236(21) ^e	2.88(30)	2 ⁻ , 3 ⁻
1951.7(7)	6247.1(7)	117(19)	6270.2(6)	170(20)	0.69(29)	i
1973.2(4)	6225.6(3)	314(19)	6246.3(9)	109(27)	2.89(74)	1 ⁻ , 4 ⁻
1983.0(4)	6215.8(3)	363(18)	6237.9(4)	211(18)	1.72(17)	{ 1 ⁻ , 4 ^{-h} 1 ⁺ , 2 ⁺ , 3 ⁺ , 4 ⁺
1999.4(5)	6199.4(5)	111(13)	6222.4(9)	87(21)	1.27(34)	2 ⁺ , 3 ⁺ (4 ⁺)
2080.1(3)	6118.7(3)	734(25)	6140.5(4)	315(19)	2.33(16)	2 ⁻ , 3 ^{-f}
2104.5(6)	6094.3(6)	119(16)	6117.0(6)	120(29) ^e	0.99(27)	2 ⁺ , 3 ⁺ (4 ⁺)
2119.7(4)	6079.1(4)	287(22)	6101.8(5)	79(12) ^e	3.63(62)	1 ⁻ , 4 ⁻
2128.3(4)	6070.5(4)	312(21)	6091.5(7)	83(21)	3.74(34)	1 ⁻ , 4 ⁻
2149.1(6)	6049.7(6)	111(20)	6072.7(7)	85(16)	1.31(34)	2 ⁺ , 3 ⁺ (4 ⁺)

^aThese reduced intensities are given in arbitrary units, normalized to a value of 100 for the primary transition feeding the first 2⁺ state in each measurement.

^bSpin and parity assignments which could be made from the current studies alone. The assignments are based on the ARC data, with the exception of a few cases where a $J^\pi=1^-$ or 4⁻ assignment could be eliminated because of population in the appropriate single resonance (see footnotes c and g).

^cPopulation from $J^\pi=2^+$ resonance at 3.68 eV was used to eliminate the $J^\pi=4^-$ assignment.

^dThe line is obscured by a contaminant at this energy.

^eThe intensity has been corrected for a contribution from a contaminant.

^fThe intensity in 24 keV indicates the possibility of an additional unresolved state with $J^\pi=1^+, 2^+, 3^+$, or 4⁺.

^gPopulation from $J^\pi=3^+$ resonance at 2.72 eV was used to eliminate the $J^\pi=1^-$ assignment.

^hThe reduced intensities indicate an unresolved doublet with the J^π values indicated.

ⁱThe reduced intensities indicate an unresolved doublet of states with J^π values of either 2⁺, 3⁺ and 1⁺, 4⁺ or 4⁺ and 4⁺.

TABLE II. High energy γ rays in ^{164}Dy observed in 2 and 24 keV capture. Errors on the last digit of the energies and intensities are given in parentheses.

E_x (keV)	2 keV		24 keV		$\frac{I_R(2\text{ keV})}{I_R(24\text{ keV})}$	$J^{\pi b}$
	E_γ (ΔE_γ) (keV)	$(I_\gamma/E_\gamma^5)^a$ (keV)	E_γ (ΔE_γ) (keV)	$(I_\gamma/E_\gamma^5)^a$ (keV)		
73.3(4)	7586.1(4)	100(5)	7608.3(4)	100(6)	1.00(7)	$2^+, 3^+$
242.3(4)	7417.2(4)	95(10) ^c	7439.3(4)	77(6)	1.23(16)	$2^+, 3^+, 4^+$
761.9(4)	6897.6(4)	112(8)	6920.0(4)	140(7)	0.80(7)	$2^+, 3^+$
828.1(4)	6831.4(4)	138(7)	6853.6(4)	97(7)	1.42(13)	$2^+, 3^+$
915.8(4)	6743.7(4)	74(5)	6766.2(5)	66(6)	1.12(13)	$4^+(1^+, 2^+, 3^+)$
976.8(5)	6682.6(4)	21(3) ^c	6704.9(5)	59(5)	0.36(6)	$2^-, 3^-, 4^-$
1038.9(5)	6620.6(5)	17(2)	6642.9(5)	71(6)	0.24(3)	$2^-, 3^-$
1123.1(5)	6536.4(5)	16(2)	6559.1(5)	43(4)	0.37(6)	$2^-, 4^-(1^-, 3^-)$
1225.9(7)			6455.8(7)	24(4)		5^-
1588.2(5)	6071.3(5)	23(3)	6093.7(6)	42(6)	0.55(11)	$2^-, 4^-(1^-, 3^-)$
1674.5(9)	5985.0(9)	11(3)	6007.5(7)	34(6)	0.32(10)	$1^-, 4^-(2^-)$
1716.0(4)	5943.5(4)	118(7)	5965.6(5)	80(7)	1.48(16)	$2^+, 3^+$
1757.8(6)	5901.6(6)	21(3)	5923.7(9)	77(19)	0.27(8)	$2^-, 3^-, 4^-(1^-)$
1796.5(4)	5863.0(4)	117(7)	5884.7(5)	91(20) ^c	1.29(29)	$2^+, 3^+$
1809.1(9)	5850.4(9)	12(3)	5871.7(9)	27(7)	0.44(16)	$1^-(4^-)$
1840.8(7)	5818.7(7)	33(4)	5841.0(11)	35(9)	0.94(27)	$2^-(3^-), 1^+$
1845.8(10)	5813.7(10)	18(4)	5835.8(9)	61(9)	0.30(8)	$2^-, 3^-, 4^-$
1852.4(4)	5807.1(4)	90(7)	5829.5(8)	51(8)	1.76(31)	$4^+(1^+, 2^+, 3^+)$
1891.7(4)	5767.8(4)	80(6)	5790.5(7)	52(7)	1.54(24)	$4^+(1^+, 2^+, 3^+)$
1909.8(6)	5749.7(6)	29(4)	5771.9(6)	72(10)	0.40(8)	$2^-, 3^-$
1921.0(4)	5738.4(4)	84(7)	5761.1(6)	79(9)	1.06(15)	$2^+, 3^+$
1933.0(4)	5726.5(4)	105(10) ^c	5748.7(6)	87(11)	1.21(19)	$2^+, 3^+$
1949.3(6)	5710.1(6)	26(4)	5733.0(8)	50(9)	0.52(12)	$2^-, 3^-(4^-), 1^+$
1978.6(4)	5680.9(4)	186(11)	5703.2(4)	214(15)	0.87(8)	$\begin{cases} 2^+, 3^+ \\ 2^+, 3^+, 4^+ \end{cases}$
1985.3(7)	5674.2(7)	27(4)	5696.3(6)	80(9)	0.34(6)	$3^-(2^-)$
2049.1(5)	5610.4(5)	106(11) ^c	5631.9(8)	134(31)	0.79(20)	$2^+, 3^+(4^+)$
2053.3(5)	5606.2(5)	107(10)	5628.5(9)	123(31)	0.87(23)	$2^+, 3^+(4^+)$
2077.9(5)	5581.6(5)	84(8)	5603.0(5)	137(14)	0.61(9)	$2^+, 3^+$
2101.5(5)	5558.0(5)	81(8)	5581.5(12)	54(18)	1.50(52)	$1^+, 2^+, 3^+, 4^+$
2112.8(5)	5546.7(5)	90(8)	5569.0(6)	81(12)	1.11(19)	$2^+, 3^+, 4^+(1^+)$
2123.7(5)	5535.8(5)	82(8)	5559.1(6)	95(13)	0.86(14)	$2^+, 3^+(4^+)$
2152.3(6)	5507.2(6)	87(12)	5528.6(7)	106(14)	0.82(16)	$2^+, 3^+(4^+)$

^aThese reduced intensities are given in arbitrary units, normalized to a value of 100 for the primary transition feeding the first 2^+ state in each measurement.

^bSpin and parity assignments which could be made from the current studies alone. The assignments are based entirely on the ARC data with the exceptions of a few cases where a $J^\pi=4^+$ assignment could be eliminated because of population from the $J^\pi=2^-$ single resonance (see footnote d).

^cThe intensity has been corrected for a contribution from a contaminant.

^dPopulation from the $J^\pi=2^-$ resonance at 1.71 eV was used to eliminate the $J^\pi=4^+$ assignment.

^eThe reduced intensities indicate an unresolved doublet, with the J^π values shown.

set of states can be guaranteed is determined by the spin and parity of the target nucleus.

As an example, in the case of the $^{163}\text{Dy}(n, \gamma)^{164}\text{Dy}$ measurement, the spin of ^{163}Dy is $\frac{5}{2}^-$, and hence s wave capture, which is the dominant process at 2 keV neutron energy, leads to capture states of 2^- and 3^- in ^{164}Dy . Final states with J^π values of 2^+

or 3^+ can then be populated via $E1$ transitions from both capture states, and will thus constitute the group with maximum reduced intensity. Transition to states with $J^\pi=1^+, 4^+$, which can be populated from only one of the capture states, should have reduced intensities approximately half that of the $2^+, 3^+$ group. Negative parity states are populated by

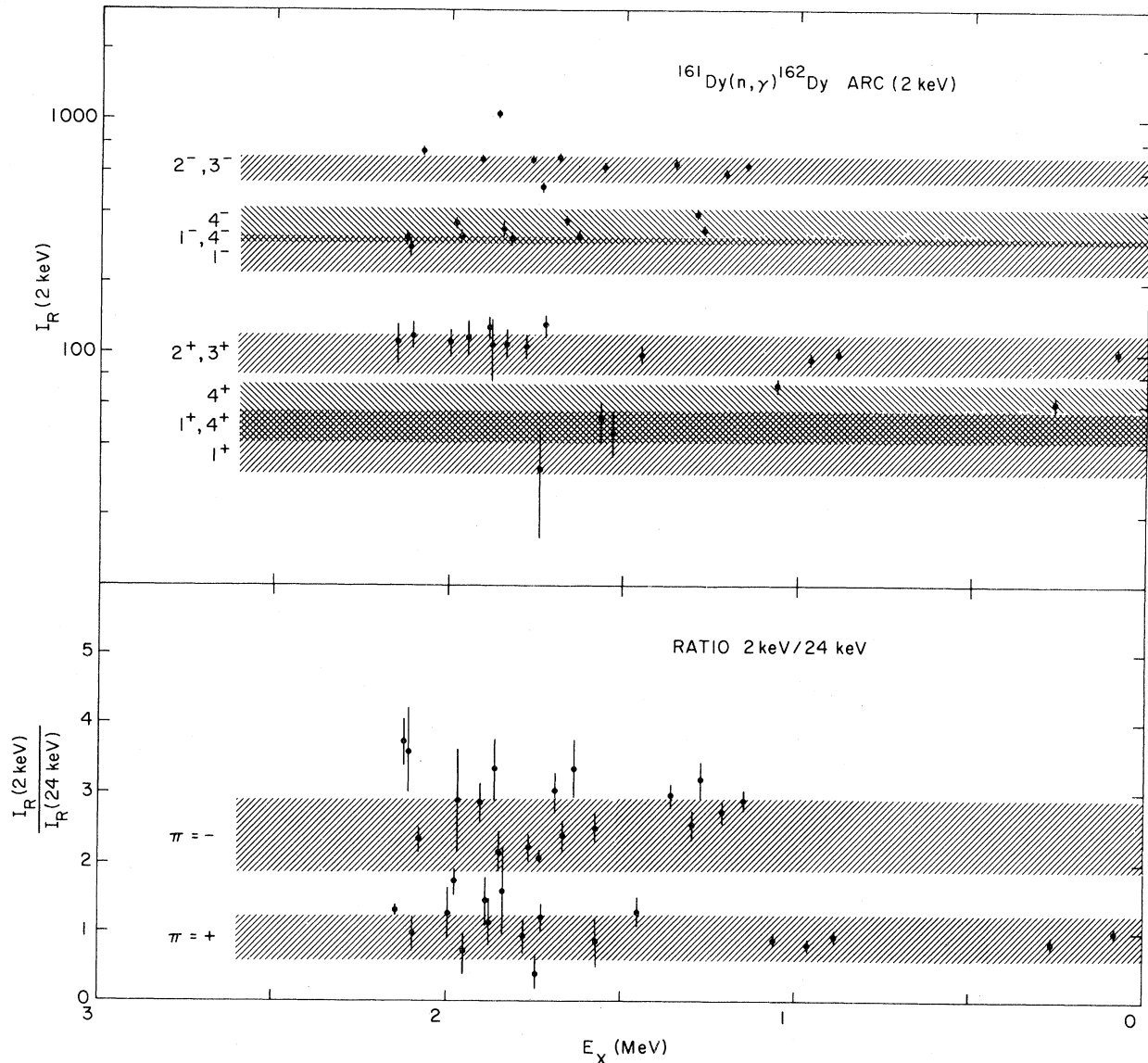


FIG. 2. (a) Reduced intensities at 2 keV from the ARC data for ^{162}Dy . The horizontal shaded bands denote the predicted $\pm 1\sigma$ spread in intensity for each J^π group. (b) The ratio of reduced intensities observed in 2 and 24 keV capture. The shaded bands correspond to the predicted $\pm 1\sigma$ spread for each parity.

$M1$ transitions, and should have a strength of approximately 0.16 that of the corresponding positive parity groups. In 24 keV capture, however, p -wave capture also becomes significant, and allows the population of negative parity states via $E1$ transitions. Thus the ratio of reduced intensities observed in 2 and 24 keV capture will serve to distinguish between the parities of the final states. Indeed, this feature is apparent in Fig. 1 where, for instance, lines 7 and 13 correspond to final states of negative parity while lines 1–5 correspond to positive parity. The increase in intensity at 24 keV of the former two lines, relative to the latter group, can be easily

seen.

In the past, the above arguments, coupled with empirical reduced intensities to final states with known J^π values, have been used to establish the intensity bands defining the different J^π values. However, Chrien⁹ has recently shown that the predicted relative means and standard deviations of the different intensity groups can be calculated rather reliably with a Monte Carlo analysis. The results of these calculations have been used in the current study to establish the J^π assignments discussed below.

The data for the two nuclei are summarized in

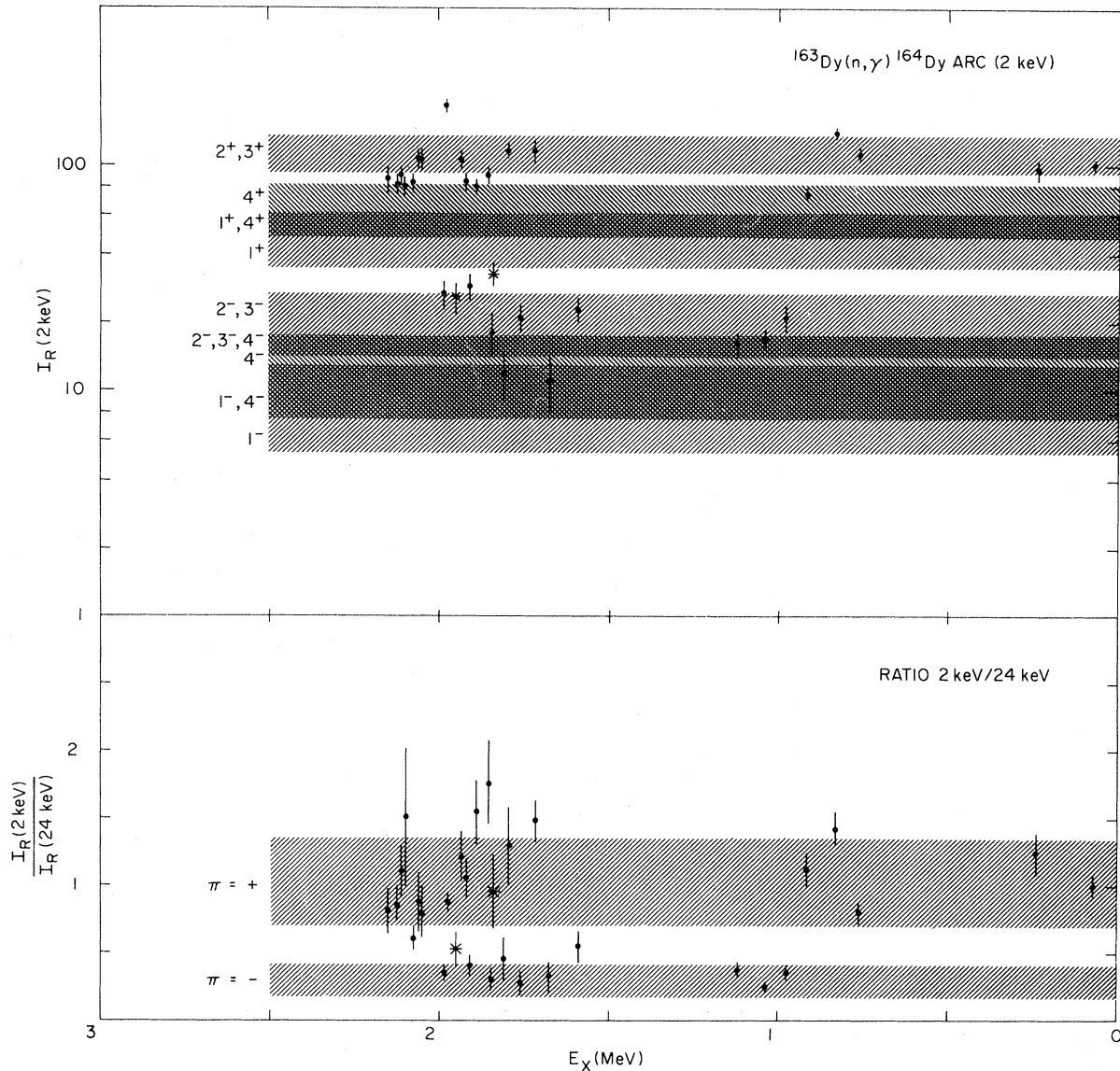


FIG. 3. Reduced intensities at 2 keV, and the ratio of 2 and 24 keV intensities for ^{164}Dy . See the caption to Fig. 2 for details. The points drawn as asterisks could not be assigned a unique parity.

Tables I and II, and the corresponding reduced intensities at 2 keV neutron energy, as well as the ratio of reduced intensities at 2 and 24 keV, are plotted versus excitation energy in Figs. 2 and 3 for ^{162}Dy and ^{164}Dy . The bands drawn on each figure correspond to the calculated ± 1 standard deviation limits for each spin category. The calculated means for the most intense groups were normalized to the data separately for each parity using the results for the first five or six states with known J^π values of 2^+ , 3^+ or 2^- , 3^- .

A number of interesting features emerge. It is

clear that the predicted fluctuations for ^{164}Dy are much larger than for ^{162}Dy . This results simply from the fact that the level density of resonances in ^{164}Dy is roughly a factor of 8 smaller than in ^{162}Dy . It can also be seen that the bands for the $J=1$ and 4 groups separate, as a result of the different spin cut-off factors which enter the Monte Carlo calculation of the ARC cross sections in each case. This feature thus represents a useful refinement over earlier ARC analyses, which assumed a single band for the $J=1$, 4 groups. In fact, this result, coupled with the larger predicted spread of intensities in ^{164}Dy , ac-

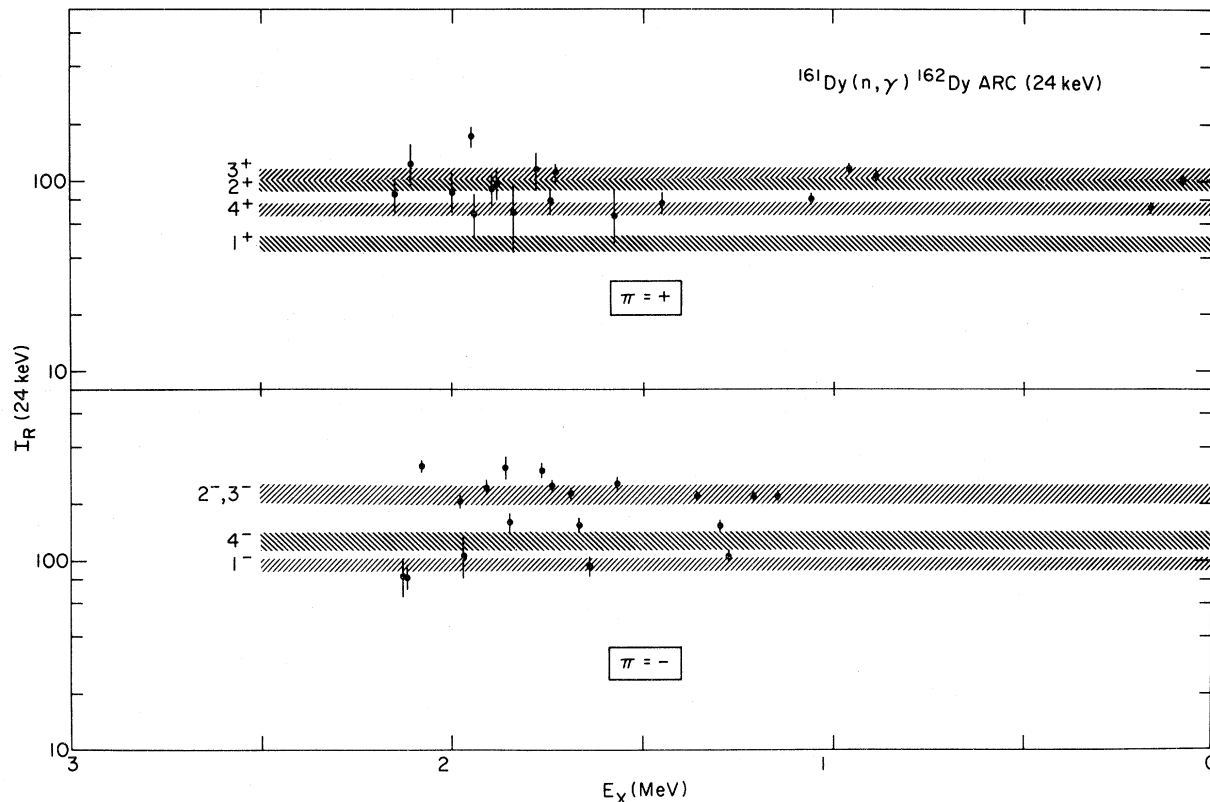


FIG. 4. Reduced intensities at 24 keV from the ARC data for ^{162}Dy , separated according to the parity of the populated state. Shaded bands denote predicted $\pm 1\sigma$ spread in intensities for each J^π group.

counts for an otherwise puzzling feature of the data for ^{164}Dy , namely, the fact that the reduced intensities of the known $J^\pi=4^+$ states do not show the factor of 2 separation from the $J^\pi=2^+, 3^+$ group expected from the simple treatment discussed earlier. In contrast, the two groups are well separated in ^{162}Dy , both empirically and in the calculations. Indeed, it can be seen that the calculations appear to predict the observed intensity groups remarkably well.

The results of Figs. 2 and 3 can therefore be used with some confidence to limit the possible J^π assignments in the two final nuclei. However, a further improvement can be introduced. In Figs. 2 and 3, and, indeed, in earlier ARC studies, the 24 keV data have been used principally to define the parities of the final states. Nevertheless, the 24 keV measurement has an inherent advantage over the 2 keV which has not, to date, been fully exploited. The larger effective averaging width of the 24 keV beam, coupled with the inclusion of p wave resonances in the averaging process, leads to significantly reduced

fluctuations in the predicted reduced intensities. The difficulty in utilizing the 24 keV data fully arises from the fact that the positive and negative parity intensity groups overlap substantially due to the influence of the p wave component. However, if the results of Figs. 2 and 3 are first used to separate the final states according to parity, the 24 keV data can be studied in more detail, as shown in Figs. 4 and 5. The smaller widths of the predicted intensity bands are immediately evident. Thus, the $J^\pi=2^+, 3^+$ and $1^+, 4^+$ states separate much more in ^{164}Dy , while in ^{162}Dy the $J^\pi=1^+$ and 4^+ groups themselves have become considerably separated.

The J^π assignments in the final column of Tables I and II result principally from the combined information of Figs. 2–5. Specifically, the preferred assignments represent instances in which the measured reduced intensities are within 2σ of the appropriate calculated intensities, where σ represents the combined error from the data and the predicted fluctuations. Assignments in parentheses correspond to cases where the difference in either case falls be-

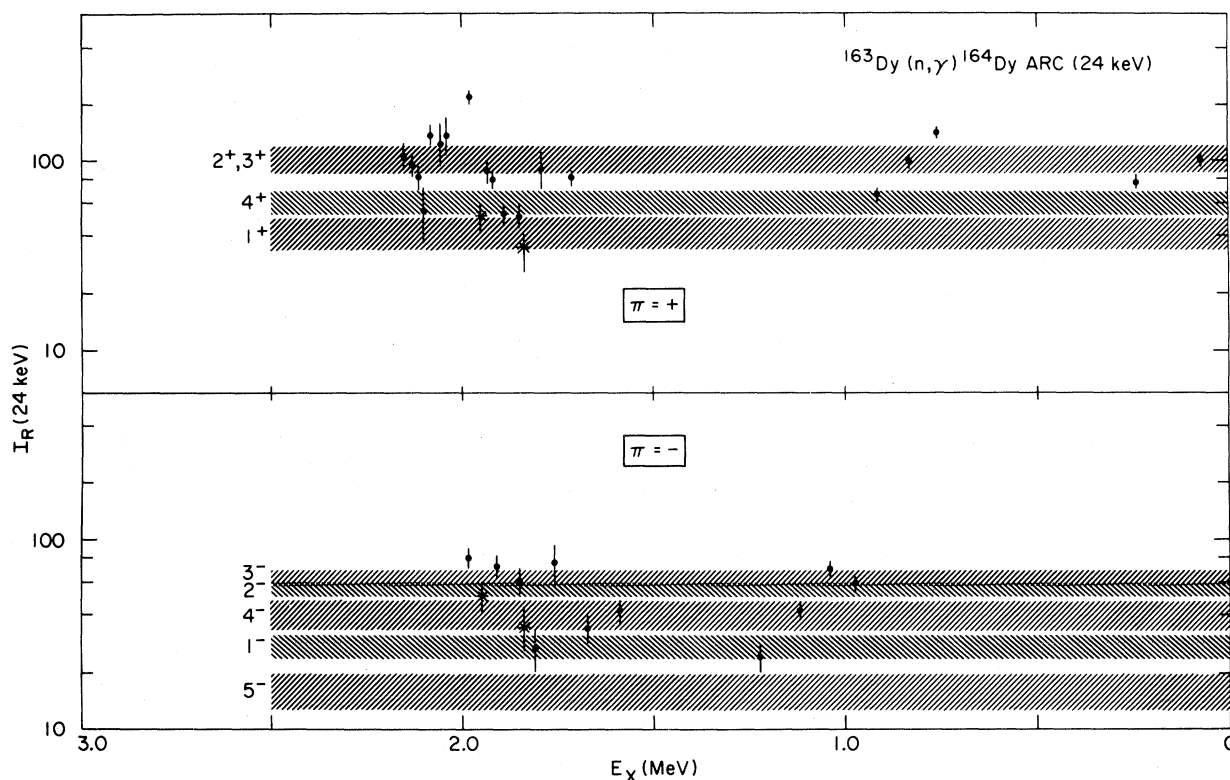


FIG. 5. Reduced intensities at 24 keV for ^{164}Dy . See the caption to Fig. 4 for details. The points drawn as asterisks are plotted in both halves of the figure, since the parity could not be uniquely determined in these cases.

tween 2σ and 3σ . In a number of cases, the combined results for a given γ ray are not consistent with any single J^π assignment. Some obvious examples of these can be seen in Figs. 2 and 3, where a number of points lie well above the maximum intensity group. Such points must therefore represent (at least) doublets and, under such an assumption, it has been possible to limit the possible J^π values of the two members in some instances. However, in this context, a limitation of the technique should be pointed out. Inspection of Figs. 2–5 shows that it is clearly possible for a doublet of lines with appropriate J^π values to produce an intensity corresponding to a single line with a different J^π value. An obvious example would be a doublet of $J=1$ or 4 levels, which would appear as a $J=2, 3$ point in both the 2 and 24 keV measurements. In addition, a combination of $J^\pi=1^+, 4^+$ and $2^-, 3^-$ in ^{162}Dy (or $1^-, 4^-$ and $2^+, 3^+$ in ^{164}Dy) would also be indistinguishable from a single $J^\pi=2^-, 3^-$ (or $2^+, 3^+$) point.

The final J^π values listed in Tables I and II were further refined by a simple analysis of the single resonance measurements. As mentioned earlier, the

primary intensities in such a case vary widely, so that the specific intensity of an individual peak has little significance. However, since a given resonance has a unique spin and parity, the *existence* of a peak frequently allows one or more of the J^π values deduced from the corresponding ARC intensities to be eliminated, essentially by inspection. In ^{161}Dy , for example, the 2.72 and 3.68 eV resonances have $J^\pi=3^+$ and 2^+ , so that states which are populated from both these resonances cannot have J^π values of 1^- and 4^- , respectively. Similarly the 1.713 eV resonance in ^{163}Dy has $J^\pi=2^-$ and hence serves to eliminate $J^\pi=4^+$ assignments.

IV. BAND ASSIGNMENTS

From the arguments of the preceding section, it is clear that the current results must disclose the complete set of negative parity states with $J=1-4$ in ^{162}Dy and of positive parity states with $J=1-4$ in ^{164}Dy , at least below 2 MeV in excitation. In fact, this guarantee of completeness can probably be extended to the $J=2, 3$ states of opposite parity in

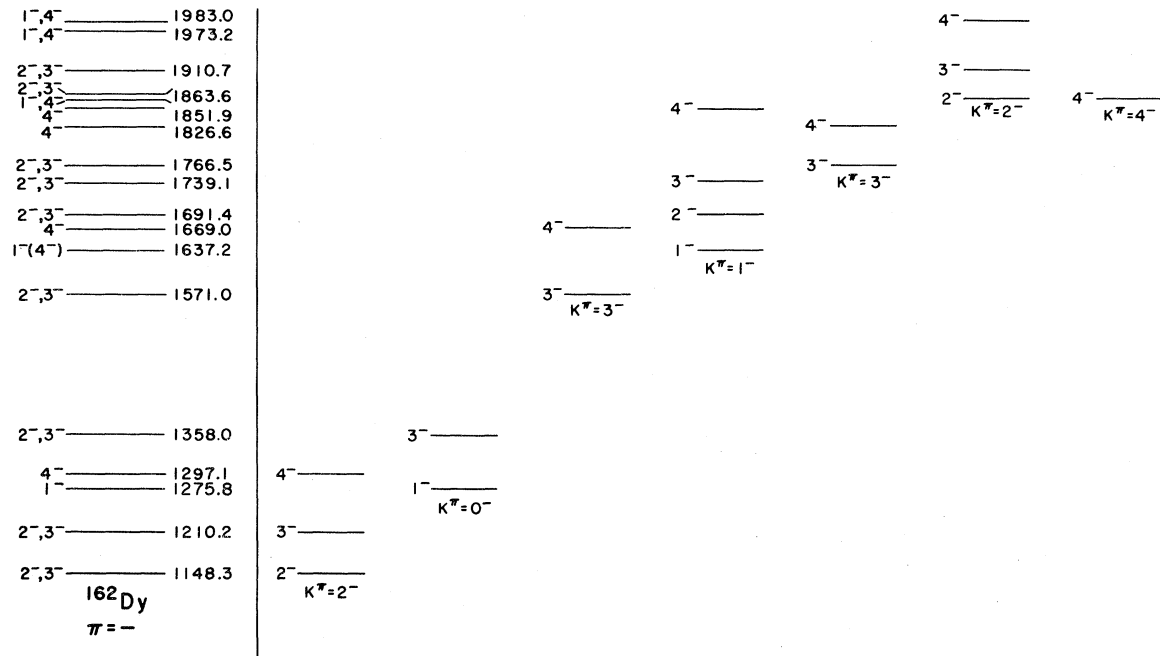


FIG. 6. Negative parity levels identified in ^{162}Dy . The left-hand side of the figure shows the levels and possible spin assignments. On the right is shown the deduced band structure. See text for details.

each case also. As pointed out in an earlier article,⁴ the knowledge that the set of states is complete leads to important additional conclusions concerning the corresponding band structure in these nuclei. In the discussion which follows, the J^π assignments in parentheses in Tables I and II, which correspond to possibilities outside the 2σ limit, have, in general, been ignored. A brief report of the results concerning the positive parity states in ^{164}Dy was presented previously.¹⁰

A. ^{162}Dy : Negative parity

The complete set of states with $J^\pi = 1^-, 2^-, 3^-$, or 4^- identified in ^{162}Dy below an excitation energy of 2 MeV is shown on the left side of Fig. 6. Considering the first two states, at 1148 and 1210 keV, each with $J^\pi = 2^-$ or 3^- , it is evident that they cannot *both* have $J^\pi = 2^-$ or 3^- , since there are not two additional 3^- or 4^- states within an energy interval consistent with a reasonable rotational spacing. The same energy argument precludes the assignment of $J^\pi = 2^-$ to the 1210 keV state. Thus the 1148 keV level must represent a $K^\pi = 2^-$ bandhead, with 3^- and 4^- rotational states at 1210 and 1297 keV, as shown. This then leaves the 1275 keV level as the next bandhead, with $J^\pi = 1^-$. Since there is only one nearby $J^\pi = 2^-, 3^-$ state, this must represent a $K^\pi = 0^-$ band and the 1358 keV level must be its 3^-

member. These bands have been proposed in earlier studies¹¹⁻¹⁴ on the basis of decay patterns, multiplicities of deexciting transitions, and (d, d') angular distributions. Higher spin members of the $K^\pi = 2^-$ and 0^- bands have recently¹⁵ been identified in the $^{160}\text{Gd}(\alpha, 2n\gamma)^{162}\text{Dy}$ reaction.¹⁵ The present results, however, by ruling out other low spin states in that energy region, *prove* that the bands must have the K values deduced above and that they are the only low K negative parity bands in this region.

The next state in Fig. 6 is at 1571 keV with $J^\pi = 2^-$ or 3^- , and must represent a bandhead, since there are no lower unassigned states. The assumption of a $K^\pi = 2^-$ assignment would require a 3^- band member within ≈ 80 keV, while the next candidate is at 1691 keV. However, the 1691 keV state is populated¹⁶ in the β decay of the ^{162}Tb 1^- ground state with a $\log ft$ value of 6.6, and hence the $J^\pi = 2^-$ assignment must be chosen for this level. Thus a $K^\pi = 3^-$ assignment seems likely for the 1571 keV level, and this conclusion is supported by the (d, d') results. The only candidate for the associated 4^- state is then seen to be at 1669 keV.

The preceding analysis leaves the 1^- 1637 keV level as a bandhead with $K^\pi = 1^-$ or 0^- . The 1739 keV level is observed in the (d, d') study and hence has $J^\pi = 3^-$. Thus, *if* the 1637 keV band has $K = 0^-$, then the 2^- 1691 keV level must be a bandhead as well, thus making two bands which must

each have 3^- members. There are, in fact, two possible candidates for 3^- rotational excitations, the aforementioned 1739 keV level and the 1766 keV state. However, the latter has itself been assigned as a $K^\pi=3^-$ bandhead in the (d,p) study of Ref. 17, so that only one 3^- rotational excitation remains, ruling out the possibility of these two bands. If, on the other hand, the 1637 keV band is taken as $K^\pi=1^-$, the 1691 and 1739 keV levels can form the 2^- and 3^- rotational excitations. The 4^- level can be the 1826 or 1851 keV level, or, perhaps, one of the two levels at 1863 keV. The (d,p) study assigned a level at ≈ 1832 keV (presumably the present 1826 keV level) as the 4^- state of the 1766 keV band. The assignment of the 1851 keV level in Fig. 6 to the 1637 keV $K^\pi=1^-$ band is then somewhat arbitrary, since the 1863 keV level might equally well have been chosen.

With the 1766 and 1826 keV levels already ascribed as the first two states of a $K^\pi=3^-$ band, this leaves a $J^\pi=1^-, 4^-$ level at 1863 keV and two $J^\pi=2^-, 3^-$ states at 1863 and 1910 keV as the next to be assigned to bands. The (d,p) study of Ref. 17 assigns a level at ≈ 1866 keV as a 2^- bandhead with 3^- and 4^- rotational states at ≈ 1913 and ≈ 1981 keV. These levels presumably correspond to the present levels at 1863, 1910, and 1983 keV. If the

other 1863 keV level (which is 1^- or 4^-) were 1^- , it would require rotational sequences of either $2^-, 3^-$, or 4^- (if $K^\pi=1^-$) or 3^- (if $K^\pi=0^-$). However, the only (see Table I) unassigned negative parity level below 2080 keV is the 1973 keV state and it cannot be 3^- . Thus the 1863 keV level is 4^- and must be a bandhead. Similarly, the $1^-, 4^-$ level at 1973 keV is also a bandhead.

B. ^{162}Dy : Positive parity

Final states with positive parity are populated via $M1$ primary transitions in ^{162}Dy and thus constitute the groups of weaker intensity. Transitions to states with $J^\pi=1^+$ or 4^+ are further reduced in intensity since they can only be populated from one of the two possible capture states, and thus completeness cannot be entirely guaranteed for such levels. Nevertheless, the ARC data for the positive parity states in ^{162}Dy , summarized in Fig. 7, allow a number of firm conclusions to be drawn concerning the associated band structure.

The ground state and gamma bands in ^{162}Dy are well established¹¹ and need no further comment. The remaining positive parity states identified below 2 MeV are shown on the left side of Fig. 7. The 2^+ state at 1453 keV must represent either a 2^+ band-

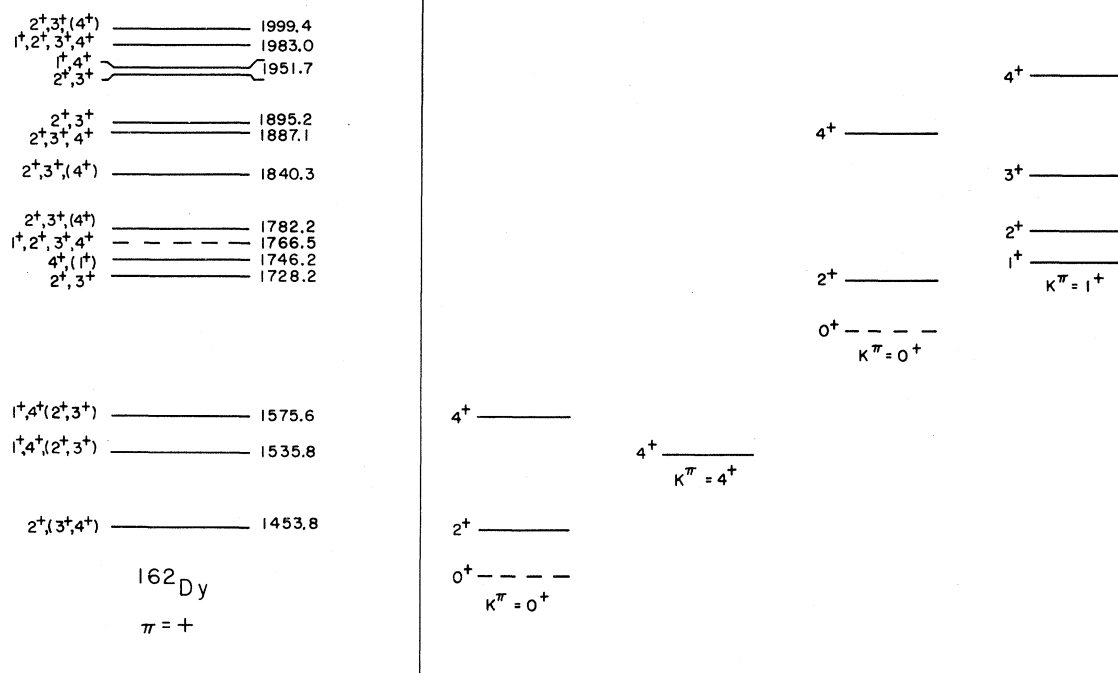


FIG. 7. Positive parity levels and deduced band structure in ^{162}Dy . The ground and γ bands are not included. The existence of the dashed level on the left is uncertain. The dashed 0^+ levels on the right are proposed bandheads which were not populated directly in ARC.

head, the 2^+ member of a 1^+ band, or the 2^+ member of a 0^+ band, since 0^+ states were not populated in the current study. It is immediately evident that there are no nearby candidates for 3^+ states, so that the former two possibilities can be ruled out. In fact, previous studies^{15,17} have identified a 0^+ state at 1400.3 keV, and suggested the 1453 keV state as the associated 2^+ state. Energy considerations then favor the level at 1575 keV as the 4^+ member of this band.

The 1535 keV state is thus left as a bandhead with $J^\pi=1^+$ or 4^+ , and since there are no nearby 2^+ states, it must be assigned $K^\pi=4^+$. The next state, a 2^+ , 3^+ level at 1728 keV, then becomes the next bandhead with $K^\pi=2^+$ or 3^+ , or the 2^+ member of a $K^\pi=1^+$ or 0^+ band. Earlier (p,t) studies¹⁸ clearly identified a 0^+ state at 1670 keV and, in fact, also populated a state at ≈ 1732 keV which can be associated with the 1728 keV state of the present work. In addition, the present data show that the next can-

didate for a 2^+ state associated with the 1670 keV bandhead is at 1766 keV, which would imply a rotational spacing twice that of the 1400 keV band. Thus the 1728 keV level can be taken to be the 2^+ member of a second 0^+ band, and the most likely candidate for the 4^+ band member lies at 1887 keV.

The next unassigned level at 1746 keV with $J^\pi=4^+$ (1^+) must therefore be the next bandhead. In this case, the preferred J^π assignment of 4^+ seems to be ruled out by the decay data,¹⁶ which show β population from the 1^- ^{162}Tb ground state. This would indicate a $K^\pi=1^+$ band based at 1746 keV, which is consistent with the results of the (d,t) studies.¹⁴ Ignoring the 1766 keV state, whose existence is not certain, the 2^+ , 3^+ , and 4^+ band members must lie at 1782, 1840, and 1951 keV, respectively. The first two of these are consistent with the less accurate energies proposed in the (d,t) work, but this earlier study suggested a level at ≈ 1906 keV as the 4^+ member, which is not con-

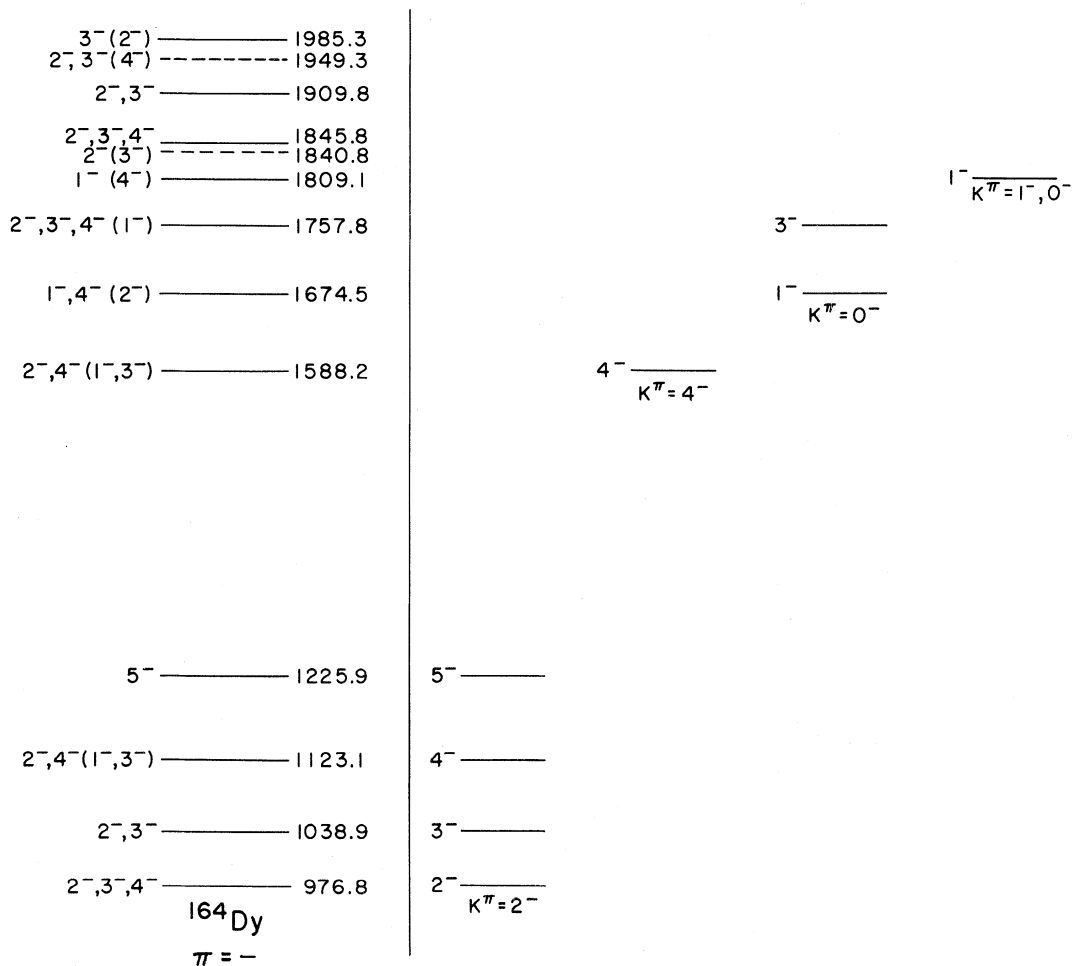


FIG. 8. Negative parity levels and deduced band structure in ^{164}Dy . The dashed lines indicate levels with two possible parity assignments.

firmed by the present results. However, as pointed out in the preceding section, it is possible that a 4^+ state unresolved from a $2^-, 3^-$ level might not be distinguished in the ARC analysis, since the former would make a very small contribution to the total intensity. Since a $2^-, 3^-$ state exists at 1910 keV, this might offer an explanation for the above disagreement.

C. ^{164}Dy : Negative parity

The negative parity s -wave capture state in ^{164}Dy implies that transitions populating negative parity final states will constitute the weaker group of reduced intensities in 2 keV capture. However, the enhanced sensitivity of the 24 keV measurement to such transitions, evident in the lower portion of Fig. 1, renders it unlikely that states with $J^\pi=2^-$ or 3^- below 2 MeV in excitation energy will have been missed. The set of negative parity states identified below 2 MeV is shown on the left side of Fig. 8.

Considering the first four levels, the current results yield an unambiguous band assignment. This can be easily seen as follows, using Fig. 8. The J^π values of the 977 and 1039 keV states are $2^-, 3^-$, 4^- and $2^-, 3^-$, respectively. Clearly, the former must represent a bandhead, since there are no low spin negative parity states at lower excitation energy. Given the firm negative parity assignments

from the current studies, the angular correlation results of Ref. 13 yield a $J^\pi=2^-$ assignment for the 977 keV level. Thus this level must represent a $K^\pi=2^-$ bandhead, and the next three levels must constitute the members of this band. These conclusions are consistent with earlier results.^{12,19-21}

The remaining negative parity states identified below 2 MeV in the present study are shown on the left side of Fig. 8 along with their preferred spin assignments from Table II. Since the data do not allow a unique determination of the parity of the 1840 keV level, it has been included as a dashed line in Fig. 8, with its associated negative parity spin assignments. The state at 1588 keV clearly constitutes either the 2^- member of a $K^\pi=1^-$ band, or a bandhead with $K^\pi=2^-$ or 4^- . The former two choices can be eliminated because the nearest 3^- state is at 1757 keV. Then the 1674 keV level also becomes a bandhead. Assuming that there are not two 4^- bands so close in energy, the most likely assignment for the 1674 keV level is $J^\pi=1^-$, indicating a band with $K^\pi=0^-$ or 1^- , with corresponding J^π values of 3^- or 2^- for the 1757 keV level. The (d,d') study of Ref. 12 shows relatively strong population of a level at 1753 keV, which was, in fact, suggested as having $J^\pi=3^-$. The absence of an intervening 2^- level then implies that the 1674 keV band has $K^\pi=0^-$. The 1809 keV level must then be a band-

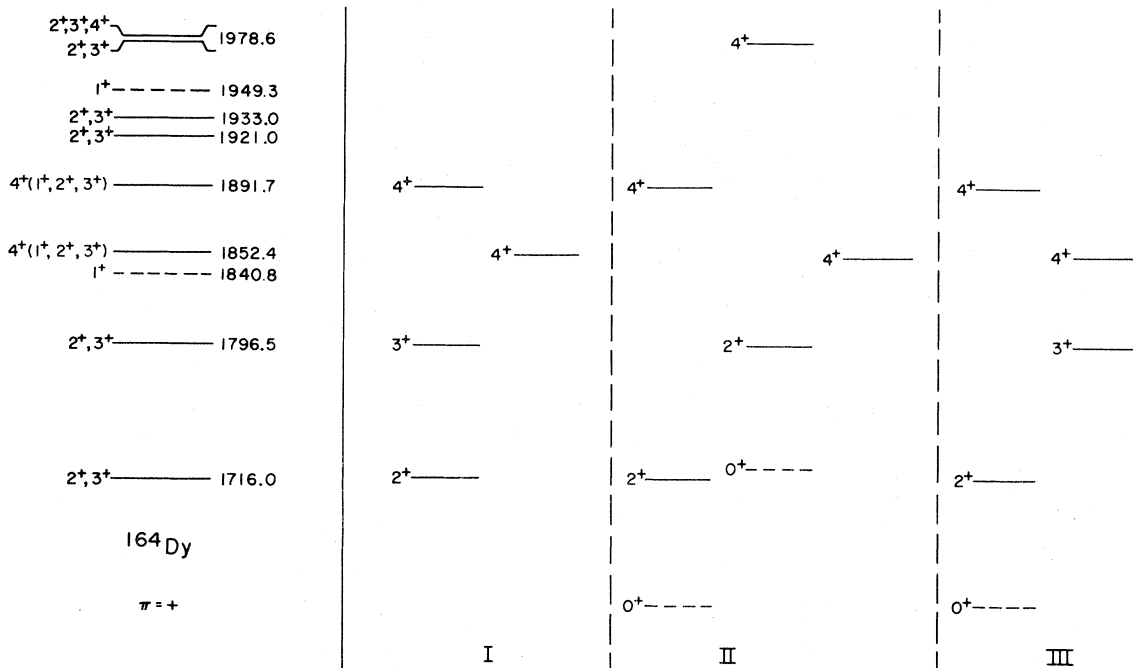


FIG. 9. Positive parity levels and deduced band structure in ^{164}Dy . The ground and γ bands are not included. The dashed lines on the left indicate levels with two possible parity assignments. Those on the right represent the approximate positions of 0^+ bandheads implied by scenarios II and III.

head, with $K^\pi=1^-$ or 0^- . While no further firm band assignments can be made, due in part to the ambiguity associated with the parity of the 1840 keV state, it is clear that there must be at least one additional low K negative parity band below 2 MeV.

D. ^{164}Dy : Positive parity

The ground and γ bands in ^{164}Dy have been well established in earlier studies,¹⁹ and thus require no further comment. The additional positive parity states identified above the γ band, and below 2 MeV, are summarized on the left side of Fig. 9. As in the previous section, the 1840 keV level has been included as a dashed line. Given the completeness below 2 MeV for $J^\pi=1^+-4^+$ states, the existence of previously proposed¹⁹ positive parity levels at 1394, 1607, and 1726 keV is ruled out by the current study. The nonexistence of the 1394 keV level is particularly significant, since it was tentatively proposed as the 2^+ member of the expected $K^\pi=0^+$ (β) band. Of course, 0^+ states are not populated directly in the ARC measurements. However, any such state must represent a bandhead, and the associated 2^+ and 4^+ band members must be populated. Thus, simple inspection of the experimental states in Fig. 8, or, indeed, the 2 keV spectrum of Fig. 1, yields the conclusion that *there are no 0^+ bands in ^{164}Dy below an excitation energy of ≈ 1630 keV*, since the first possible 2^+ state lies at 1716 keV, and the 2^+ energy in the ground band is 80 keV. Certain other important inferences can be drawn from the known completeness of the observed set of states. Considering the $J^\pi=2^+, 3^+$ states at 1716 and 1796 keV, it is unlikely that they both constitute $K^\pi=3^+$ bandheads. The possibility that they both represent $K^\pi=2^+$ bandheads would require a $J^\pi=3^+$ state within ≈ 100 keV of each level, while the ARC results show that the nearest candidate lies at 1921 keV. If the 1716 keV state were a $K^\pi=3^+$ bandhead, then the same energy argument precludes the 1796 keV level being a $K^\pi=2^+$ bandhead. Thus the most likely solution is that the 1716 keV level has $J^\pi=2^+$, and represents either the 2^+ member of a $K^\pi=0^+$ band, or a $K^\pi=2^+$ bandhead. These considerations lead to the three suggested band structures involving these levels, illustrated on the right side of Fig. 9. It can be seen that scenarios I and III can be distinguished from II by virtue of the spin of the 1796 keV state, which is 3^+ in the former two instances, and 2^+ in the latter. It is interesting to note that, in the (d, d') study of Ref. 12, a state at 1791 keV is weakly populated. If this state corresponds to the 1796 keV level in Fig. 8, it would point to scenario II as the correct solution, since only natural parity states are directly populated in

the (d, d') reaction. Finally, it can be remarked that, if the 1840 keV level has positive parity, it must constitute a $K^\pi=1^+$ bandhead.

V. DISCUSSION

A. Positive parity structure

The $K^\pi=1^+$ and 4^+ bands at 1746 and 1535 keV in ^{162}Dy have been discussed in earlier studies.¹⁴ The former was assigned as the $\frac{3}{2}[521]-\frac{5}{2}[523]$ two neutron configuration on the basis of the observed relative (d, t) cross sections. This assignment was also supported¹⁶ by the $\log ft$ ratio for β transitions to the 2^+ and 1^+ members of this band. As pointed out in the previous section, the current study also confirms this band, but suggests a different location for the 4^+ band member. The $J=4, 5, 6,$ and (tentatively) 7 members of the 4^+ band were also observed in the (d, t) measurements¹⁴ and later confirmed in the $(\alpha, 2n\gamma)$ study of Ref. 15. The observed relative (d, t) cross sections were consistent with an assignment of the $\frac{3}{2}[521] + \frac{5}{2}[523]$ two neutron state for this bandhead. Nevertheless, the fact that this band lies at approximately twice the γ band energy raises the question of what, if any, component can be attributed to the $K=4^+$ 2γ -phonon vibration. Indeed, the question of the identification of 2 phonon excitations in deformed nuclei has recently received considerable attention. Dumitrescu and Hamamoto²² attempted to explain the lack of a 4^+ band in ^{168}Er at twice the γ band energy by incorporating large anharmonicities in the γ motion, but met with only limited success. Soloviev and Shirikova,²³ on the other hand, have suggested that collective two phonon excitations in deformed nuclei should not be observed, since blocking effects will result in their major components being shifted 1–2 MeV higher in energy. The experimental signature of a 2 phonon band must be the $E2$ strength to the corresponding one phonon band, relative to the one phonon to ground strength. In the limit of harmonic vibrations, the intrinsic $E2$ matrix element connecting the $K=4^+$ (2γ) band to the γ band should equal that between the γ and ground bands. Note, however, that the fact that the $K^\pi=4^+$ band decays primarily to the γ band is of little significance, since transitions to other lower bands are generally K forbidden. In the present case, however, an estimate of the absolute strength of the branch to the γ band was made by Backlin *et al.*,¹⁴ using an interband-to-intraband branching ratio, which implied an $E2$ matrix element about three times smaller than that between the γ and ground bands. The corresponding $B(E2)$ value, $\approx 1.7 \times 10^{-3} e^2 b^2$, can, in fact, be accounted for by the proposed two neu-

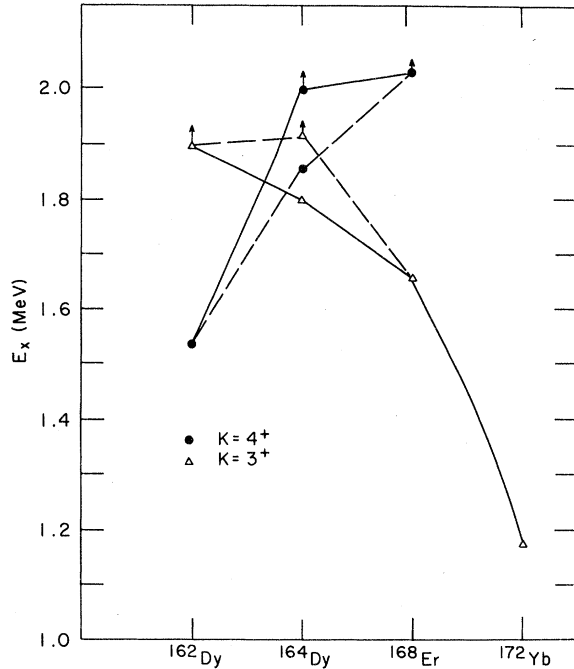


FIG. 10. Systematics of $K^\pi=3^+$ and 4^+ bandhead energies. The dashed and solid lines correspond to the different possible positions of these bandheads in ^{164}Dy (see Fig. 9). Vertical arrows correspond to lower limits.

tron configuration, using the wave functions of Bes *et al.*²⁴ for the γ band. Thus it would appear likely that the 4^+ band at 1535 keV in ^{162}Dy does not contain any appreciable component of the 2γ phonon vibration, which must then be at an energy >2.0 MeV, as was found in ^{168}Er .⁵ In ^{164}Dy the lowest candidate for a $K^\pi=4^+$ band (see Fig. 9) lies at 1852 keV, which can be compared to the γ band energy of 761 keV.

The location of $K^\pi=4^+$ and 3^+ excitations is important in light of recent interest in the possibility of hexadecapole modes of collective excitations in this region. Indeed, in this context, Walker *et al.*²⁵ recently discussed the rather extensive systematics for $K^\pi=3^+$ bands in some detail. The existing systematics for both types of band are shown in Fig. 10 for those nuclei where ARC results are known. Despite the uncertainties in ^{164}Dy , the systematics clearly show an inversion of order, with the 4^+ excitation lowest for lighter masses and the 3^+ lowest for the heavier nuclei. It is possible to provide a rather simple interpretation of this feature in terms of the possible two quasiparticle combinations that can yield 3^+ and 4^+ bands. Inspection of the Nilsson diagram shows that, in this region, the lowest $K=3^+$ excitations are most likely composed of the $\frac{7}{2}[404]-\frac{1}{2}[411]_{\pi}$, $\frac{5}{2}[402]+\frac{1}{2}[411]_{\pi}$,

$\frac{5}{2}[512]+\frac{1}{2}[521]_{\nu}$, and $\frac{7}{2}[514]-\frac{1}{2}[521]_{\nu}$ two quasiparticle states. In each case these are particle-like excitations and thus should drop in energy with increasing mass. On the other hand, as pointed out earlier, the lowest $K^\pi=4^+$ excitation in ^{162}Dy is the $\frac{5}{2}[523]+\frac{3}{2}[521]_{\nu}$ configuration. Since this is a hole excitation [confirmed by the absence of (d,p) population], it should rise in energy with increasing mass, again consistent with the systematics in Fig. 10. Alternately, correlated $K^\pi=3^+$ and 4^+ excitations can arise in the IBA with the introduction of a g boson: the emerging systematics and inversion of order presented here may be useful in constraining the parameters of such a degree of freedom.

Turning now to the 0^+ bands in the two nuclei, the most striking feature to emerge from the current work is the *lack* of any such band in ^{164}Dy , up to an excitation energy of at least 1630 keV. In contrast, two 0^+ bands have been identified in ^{162}Dy , the lowest being at 1400 keV. It was recently pointed out³ that the characteristics of the first excited 0^+ excitation in the majority of deformed rare earth nuclei are not those traditionally expected of a β vibration. Specifically, these bands exhibit very weak $B(E2)$ strengths to the ground band and, where measured, relatively strong branches to the γ band. However, these features arise naturally in the framework of the interacting boson approximation (IBA) of Arima and Iachello.² Thus the properties of the first 0^+ excitation are a question of considerable current interest. Conventional wisdom would conclude that such excitations can only be considered "collective" if they are connected by strong (similar to $\gamma \rightarrow g$) $E2$ branches to the ground band. Yet the IBA, which offers a description of collective states, predicts very weak strengths for the same transitions.

It is therefore of interest to consider the systematics of some of the empirical properties of the first 0^+ bands in deformed nuclei. Since the γ excitation is remarkably stable in terms of both energy and $B(E2)$ strength to the ground band throughout the deformed region, it is most useful to look at the energies and $B(E2)$ strengths of the 0^+ bands *relative* to the γ band, and this is done for Dy and Er in Fig. 11. The choice of ratios plotted is particularly useful in considering the application of the IBA to this problem, as will be seen below. Note that the energy ratio specified eliminates the rotational contribution to the γ bandhead energy, while both numerator and denominator in the $B(E2)$ ratio involve the squares of Clebsch-Gordan coefficients with identical values. Thus, these ratios allow a comparison of the properties of the *intrinsic* excitations in each case.

Several features are evident in Fig. 11. The energies of the first 0^+ excitations in both Dy and Er

rise near midshell, while the $B(E2)$ values drop. The $B(E2)$ ratios are for the most part in the range of ≈ 0.1 to 0.01 , indicating that, relative to the γ band, the 0^+ bands are very weakly connected to the ground band. The microscopic origin of β vibrations in deformed nuclei has been linked²⁶ to the occurrence of low lying Nilsson single particle orbits with different quadrupole moments. The largest differences, and thus the lowest lying β mode, will occur in regions where orbits from different major shells cross near the Fermi surface. This picture then seems to provide a qualitative explanation for the energy systematics of Fig. 11 in light of the known $\Delta N=2$ crossings of $N=6$ and 4 neutron orbits around $N=90$, and those expected at the upper end of the shell, between $N=7$ and 5 orbits. Nevertheless, the small size of the $\beta \rightarrow g$ $B(E2)$ values still remains contrary to the expectations of a quadrupole shape oscillation.

In the framework of the IBA the empirical systematics may be considered in terms of the simple Hamiltonian proposed in Ref. 27, viz.,

$$H = -\kappa Q \cdot Q - \kappa' L \cdot L, \quad (1)$$

where

$$Q = (s^\dagger \tilde{d} + d^\dagger s)^{(2)} + (\chi_Q / \sqrt{5})(d^\dagger \tilde{d})^{(2)}. \quad (2)$$

As pointed out in Ref. 27, since the $L \cdot L$ term is diagonal, all relative $B(E2)$ values and relative intrinsic excitation energies in this framework are uniquely specified for a given boson number N by the parameter χ_Q , which defines the structure of the quadrupole operator. Thus the relative predicted

properties of the 0^+ and γ excitations can be plotted as a function of χ_Q and N , and this is done for the energy and $B(E2)$ ratios of Fig. 11 in Fig. 12. The χ_Q values appropriate to deformed nuclei can easily be obtained from the empirical ratio

$$B(E2; 2\gamma^+ \rightarrow 0_g^+) / B(E2; 2g^+ \rightarrow 0_g^+).$$

Given the aforementioned stability of the γ mode throughout this region, this yields²⁷ a narrow range of values between $\chi_Q \approx -0.095$ and -1.25 for the Dy and Er isotopes, the corresponding boson numbers varying from 13 to 17.

A comparison of Figs. 11 and 12 now yields several interesting conclusions. The range of χ_Q and N values mentioned above corresponds to values of the energy ratio between 1.5 and 1.75, and of the $B(E2)$ ratio between 0.004 and 0.02. Thus the simple Hamiltonian of Eq. (1) provides a remarkably good quantitative description for several of the nuclei on both sides of the maximum energy ratio in Fig. 11. Moreover, the discrepancies for the nuclei with low A can be understood in terms of the onset of the transition towards a spherical shape. Previous work²⁸ has shown that the features of this transition, including the lowering of the excitation energy of the first 0^+ band, can be well reproduced in the framework of an $SU(3)$ to $SU(5)$ transition in the IBA. Such a description, however, requires the inclusion of at least one additional term in the IBA Hamiltonian, of the form ϵn_d .

One feature of the empirical trends is nevertheless clearly outside the scope of the proposed IBA Ham-

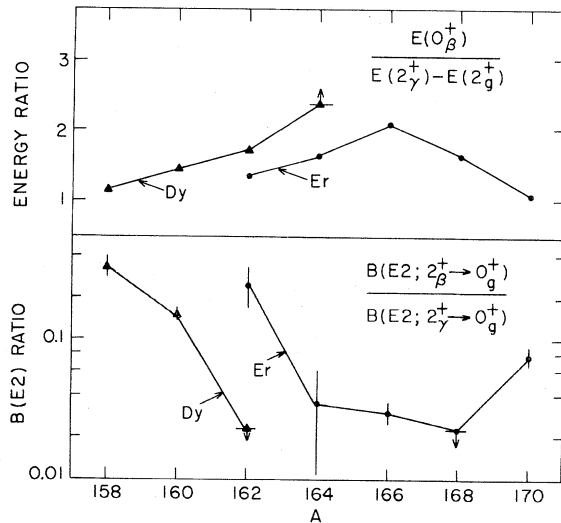


FIG. 11. Systematics of the energy and ground state $B(E2)$ value of the first 0^+ excitation, relative to the γ band, in Dy and Er nuclei. Vertical arrows indicate that the empirical values plotted represent upper or lower limits.

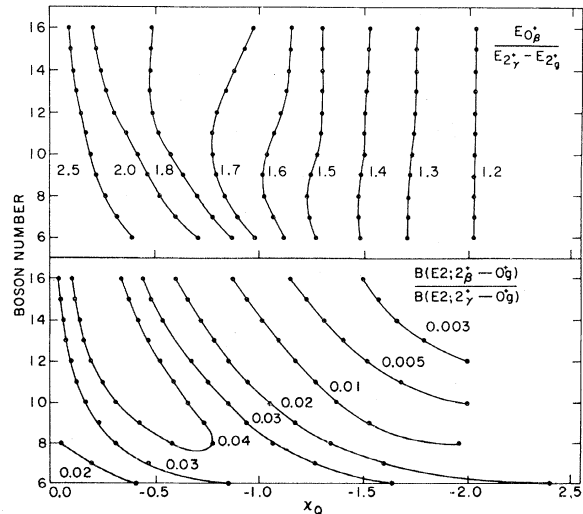


FIG. 12. Calculated contour plots of the energy and $B(E2)$ ratios of Fig. 11 versus the parameters χ_Q and N of the IBA Hamiltonian of Eq. (1).

iltonian, namely, the maximizing of the 0^+ excitation energy around midshell. Inspection of Fig. 12 shows that there is very little boson number dependence in the predicted energy ratio. Moreover, the empirical magnitudes of the energy ratios at the peaks in both Dy and Er are outside the range of the predictions for the expected χ_Q values. Although the Hamiltonian of Eq. (1) is, of course, a very simple one, and was only intended as a starting point in any detailed calculation of a deformed nucleus, the above discussion nevertheless indicates that it will be necessary to introduce a substantial change in the theoretical description of ^{164}Er and ^{164}Dy , relative to the neighboring isotopes. One caveat should be borne in mind regarding the data of Fig. 11. While the nuclei $^{162,164}\text{Dy}$ and ^{168}Er have been studied via the ARC technique, with the associated guarantee that no states have been missed at these excitation energies, this is not true for the other nuclei of Fig. 11. In general, however, the use of several different reactions to study these nuclei including, most importantly, two neutron transfer, makes it unlikely that a low lying 0^+ excitation has been missed.

In concluding this section, one further comment can be made. It might be suggested, on the basis of the weak $B(E2)$ branches to the ground band, that the 0^+ excitations discussed above should not be considered collective, but rather as two quasiparticle excitations and therefore outside the basis of collective models. However, it must be remembered that collectivity in general refers to a coherence in structure and not to the magnitude of any particular matrix element. Moreover, several specific arguments against a noncollective interpretation can be made. Firstly, the empirical systematics of Fig. 11 show a clear correlation between the energies and ground state $B(E2)$ strengths of the 0^+ excitations. Such a link can be understood naturally in a collective framework in terms of the mass and stiffness parameters associated with the intrinsic excitation. There is, however, no reason to assume *a priori* that there should be any such correlation associated with two quasiparticle excitations across the region. Secondly, the quantitative success of the simple IBA Hamiltonian of Eq. (1) for many of the nuclei considered shows that a collective basis can, in fact, explain the observed characteristics. Thus the criterion of a strong $B(E2)$ link with the ground band as a *necessary* signature of collectivity is negated. Such a criterion applies only to the assumed specific collective structure of a β (or γ) excitation and not to all possible collective excitations. Thirdly, two quasiparticle 0^+ excitations in deformed nuclei must be constructed from two different Nilsson orbits with identical K^π values. Within a given shell there are few candidates and the spacing between such or-

bits is likely to be large because of their mutual repulsion. Thus the resultant two quasiparticle excitations would be expected in general at higher energies than two quasiparticle bands with nonzero K values. Finally, the absolute $B(E2)$ values between the 0^+ and ground bands in these nuclei, while small, are still too large to be explained by the available two quasiparticle orbits in the region. This can be seen as follows. Since a pure two quasiparticle configuration is composed of a pair of particles in two *different* Nilsson orbits, while the ground state is represented by a coherent sum of pairs of particles in *identical* (time reversed) orbits, the transition matrix element between them must consist of two contributions of the form $A \rightarrow B$ and $B \rightarrow A$, where A and B represent the two orbits making up the two quasiparticle configuration. An estimate of the maximum possible value of the corresponding transition probability can therefore be obtained by summing these two contributions. For the possible Nilsson orbits which could play a role, this yields a maximum value of $0.00018 e^2 b^2$, which can be compared to the observed $\beta \rightarrow g$ transition strengths of $\approx 0.003-0.03 e^2 b^2$. Note that the above estimate neglects a number of factors which would serve to reduce the strength further, such as pairing factors and the wave function amplitudes and phases in the ground band.

B. Negative parity structure

In considering the negative parity structure exhibited in $^{162,164}\text{Dy}$, it is of interest to attempt to isolate the subset of collective octupole excitations. As pointed out in an earlier study⁵ of ^{168}Er , such a separation is not always clear-cut, since the microscopic structure of such excitations frequently incorporates only a few significant two quasiparticle components. Thus, in general, the octupole excitations in this region can be expected to be populated in both inelastic scattering experiments and single particle transfer reactions. Moreover, although the observation of enhanced $B(E3)$ strength to the ground band is a signature of a collective excitation, it is again not a necessary one, since calculated $B(E3)$ values vary considerably according to the specific structure of the particular excitation, and because of the effects of Coriolis coupling between the intrinsic excitations. With these points in mind, and using as a basis for discussion the results of microscopic calculations for collective²⁹ and two quasiparticle³⁰ negative parity excitations in these nuclei, it is possible to offer a plausible description of the observed bands.

The lowest negative parity excitation in both nuclei is a $K^\pi=2^-$ band, and in both cases the 3^-

band member is strongly connected to the ground state. Recent Coulomb excitation measurements²⁰ yield $B(E3)$ values of 9.6 and 7.9 single particle units (s.p.u.) for the 1210 and 1038 keV levels in ^{162}Dy and ^{164}Dy . This is in agreement with the calculations of Neergard and Vogel,²⁹ who predict the lowest collective octupole band to have $K^\pi=2^-$ for these nuclei, and to appear at an energy of about 1200 keV in each case. The dominant two quasiparticle component in this band can be expected³⁰ to be the $\frac{3}{2}[411]-\frac{7}{2}[523]$ two proton configuration, which explains the strong β transition from the ^{162}Tb ground state.¹⁶

A $K^\pi=0^-$ band has been identified in each nucleus at energies of 1275 and 1674 keV in ^{162}Dy and ^{164}Dy , respectively. In both cases, the associated 3^- states are populated relatively strongly in (d,d') ,¹² with $B(E3)$ values of 2.5 and 3.0 s.p.u., respectively, suggesting a collective character. The predicted energies of the 0^- bands in the calculations of Neergard and Vogel are in good agreement with the empirical ones, and nicely reproduce the shift to higher energy in ^{164}Dy . The (d,p) cross sections observed¹⁴ in ^{162}Dy indicate that a significant component of the 0^- bands must be the $\frac{5}{2}[642]-\frac{5}{2}[523]$ two neutron configuration.

A $K^\pi=1^-$ band has been found for the first time in ^{162}Dy , at an energy of 1637 keV. A state at ≈ 1741 keV was tentatively assigned as 3^- in the (d,d') study of ^{162}Dy , and this state can now be associated with the 3^- band member at 1739 keV in the present work. In ^{164}Dy , a $K^\pi=1^-$ bandhead has been identified at 1809 keV, but the next suggested candidate for a 3^- state in the (d,d') experiments lies at ≈ 2150 keV, which seems too high to be associated with the 1809 keV bandhead. A more likely possibility might be the state seen more weakly in (d,d') at ≈ 1906 keV, which could be associated with the 1909 keV $J^\pi=2^-, 3^-$ state. A major two quasiparticle amplitude in the collective $K^\pi=1^-$ band is likely to be the $\frac{5}{2}[642]-\frac{3}{2}[521]$ neutron configuration, which is predicted to be the lowest pure 1^- two quasiparticle state in the calculations of Gallagher and Soloviev.³⁰

The $K^\pi=3^-$ band is predicted²⁹ to be the least collective of the octupole excitations. It is thus not surprising that neither of the 3^- bandheads found in ^{162}Dy were assigned as 3^- states in the (d,d') study. However, a state at ≈ 1575 keV was weakly populated, and can therefore be tentatively associated with the 1571 keV bandhead. In fact, the measured cross section is consistent with the predicted $B(E3)$ values of Neergard and Vogel of 0.2 s.p.u. While no firm $K^\pi=3^-$ assignment could be made in ^{164}Dy , it can be seen in Fig. 8 that there are candidates for such a bandhead below 2 MeV.

Finally, the $K^\pi=4^-$ bandheads at 1863 and 1588 keV in ^{162}Dy and ^{164}Dy must be assigned as two quasiparticle excitations, and the lowest candidates are predicted³⁰ to be the $\frac{3}{2}[651]+\frac{5}{2}[523]$ and $\frac{5}{2}[642]+\frac{3}{2}[521]$ two neutron configurations. However, the latter would be expected to lie above the corresponding singlet configuration ($K^\pi=1^-$) and hence is unlikely to represent the dominant amplitude, at least in the case of ^{164}Dy , where the first candidate for a 1^- band lies at 1809 keV. The $K^\pi=3^-$ and 2^- bands at 1766 and 1863 keV in ^{162}Dy were both populated strongly in the (d,p) study,¹⁴ and assigned as the $\frac{5}{2}[642]\pm\frac{1}{2}[521]$ neutron configurations, which are predicted to appear around 2.3 MeV.

It has thus been possible to offer a rather complete description of the negative parity structure in $^{162,164}\text{Dy}$, and, with the exception of the $K^\pi=3^-$ band in ^{164}Dy , to identify the complete subset of collective octupole excitations. The calculations of Neergard and Vogel²⁹ are remarkably successful in reproducing the overall characteristics of the collective bands, including their relative $B(E3)$ strengths to the ground band. However, the predicted staggering in the $K^\pi=1^-$ band in ^{162}Dy is too large, resulting from the fact that the predicted 0^- band energy is about 200 keV too high, and thus generates too strong a Coriolis mixing with the $K^\pi=1^-$ band. In addition, the 3^- band is predicted to be well above the 1^- band, at ≈ 1950 keV, while experimentally it is found slightly below. In ^{164}Dy , the observed ordering of the 0^- and 1^- bands is inverted relative to the predictions.

VI. CONCLUSIONS

The current study illustrates the power of the ARC technique in nuclear structure studies. Despite the lack of information from secondary γ rays, it was possible to extend considerably the characterization of the negative and positive parity band structure in ^{162}Dy and ^{164}Dy , simply by virtue of the knowledge that the observed set of low spin states in each case is complete within a given range of excitation energy. The ability to assign specific J^π values has been put on a semiquantitative basis by use of the results of the Monte Carlo analysis of Ref. 9, and it was shown that this approach then allows the better averaging inherent in the 24 keV data to be used to further limit the J^π values. Single resonance measurements have also proved useful in eliminating possible spin assignments in a few cases.

Apart from the deduced band structure, the implied completeness of the level schemes has certain important consequences *per se*. For instance, it has been pointed out that the knowledge that there are

no 0^+ bands in ^{164}Dy below 1630 keV has important implications for the application of the IBA to this nucleus. The data also reveal that there are no candidates for a $K^\pi=4^+ 2\gamma$ phonon excitation near the expected energy in these nuclei. This conclusion has also been reached for ^{168}Er , from a similar study,⁵ and thus confirmation may be emerging of the suggestion²³ that the main components of the two phonon excitations in deformed nuclei are shifted to higher energies and considerably fragmented. In considering the negative parity structure, the absence of the even spin band members has allowed an unambiguous identification of the $K^\pi=0^-$ band in each nucleus. The identification of the complete set of collective octupole excitations again complements the results of the ^{168}Er study and it can be hoped that further investigations of this type will eventually lead to a better understanding of the behavior of these excitations across the region of deformed nuclei.

In conclusion, while the current results have been obtained solely from primary γ -ray measurements, it is, of course, essential to obtain detailed information on the secondary γ rays in order to make a detailed comparison with theoretical predictions. Such data are of particular importance in understanding the different characteristics predicted for the first 0^+ excitations in the IBA and geometrical bases. While it was emphasized in the previous section that one essential difference involves the $B(E2)$ strength to

the ground band, another equally important difference centers on the branch to the γ band, which is predicted to be of the same order as the $\gamma \rightarrow g$ strength in the IBA, but is forbidden in the limit of harmonic β and γ vibrations in the geometrical model. Such transitions have been observed in several nuclei but since they are strongly hindered by the E_γ^5 factor inherent in the $E2$ transition probability, they are difficult to detect and further experimental efforts are necessary to study this question.

In this context, it is interesting to ask whether existing²⁴ microscopic, random-phase approximation (RPA) band, wave functions would yield $\beta \rightarrow \gamma$ transition strengths similar to those predicted by the IBA. Since the published wave functions do not include phases, it is not possible to answer this question definitively. Nevertheless, it can be remarked that the magnitudes of the individual components which contribute to the total $\beta \rightarrow \gamma$ transition matrix element are ≈ 0.4 single particle units (s.p.u.), and hence sufficient to produce a matrix element ≈ 1 s.p.u. as predicted in the IBA. Thus a formal calculation of this type would be of considerable value.

ACKNOWLEDGMENTS

One of us (W.G.) would like to thank BNL for the support obtained during his visit to this institute. This research was performed under Contract DE-ACo2-76CH00016 with the United States Department of Energy.

¹D. D. Warner, R. F. Casten, and W. F. Davidson, Phys. Rev. C **24**, 1713 (1981).

²A. Arima and F. Iachello, Ann. Phys. (N.Y.) **99**, 253 (1976); **111**, 201 (1978); **123**, 468 (1979).

³D. D. Warner and R. F. Casten, Phys. Rev. C **25**, 2019 (1982).

⁴R. F. Casten, D. D. Warner, and W. F. Davidson, Phys. Rev. Lett. **45**, 1077 (1980).

⁵W. F. Davidson, D. D. Warner, R. F. Casten, K. Schreckenbach, H. G. Borner, J. Simic, M. Stojanovic, M. Bogdanovic, S. Koicki, W. Gelletly, G. B. Orr, and M. L. Stelts, J. Phys. G **7**, 455 (1981); **7**, 843 (1981).

⁶M. L. Stelts and J. C. Browne, Nucl. Instrum. **133**, 35 (1976).

⁷M. L. Stelts and R. E. Chrien, Nucl. Instrum. **155**, 253 (1978).

⁸W. R. Kane et al., *Proceedings of the International Symposium on (n, γ) Spectroscopy* (IAEA, Vienna, 1969).

⁹R. E. Chrien, *Proceedings of the Fourth International Symposium on Neutron Capture Gamma-Ray Spectroscopy and Related Topics, Grenoble, France*, IOP Conf. Series No. 62 (Institute of Physics and Physical Society,

London, 1981), p. 342.

¹⁰D. D. Warner and R. F. Casten, *Proceedings of the Fourth International Symposium on Neutron Capture Gamma-Ray Spectroscopy and Related Topics, Grenoble, France*, IOP Conf. Series No. 62 (Institute of Physics and Physical Society, London, 1981), p. 224.

¹¹A. Buyrn, Nucl. Data Sheets **17**, 97 (1976).

¹²T. Grottdal, K. Nybo, T. Thorsteinsen, and B. Elbek, Nucl. Phys. **A110**, 385 (1968).

¹³P. Hungerford, W. D. Hamilton, S. M. Scott, and D. D. Warner, J. Phys. G **6**, 741 (1980).

¹⁴A. Backlin, A. Suarez, O. W. B. Schult, B. P. K. Maier, U. Gruber, E. B. Shera, D. W. Hafemeister, W. N. Shelton, and R. K. Sheline, Phys. Rev. **160**, 1011 (1967).

¹⁵C. A. Fields, K. H. Hicks, R. A. Ristinen, F. W. N. deBoer, P. M. Walker, J. Borggreen, and L. K. Peker, Nucl. Phys. **A389**, 247 (1982).

¹⁶K. Kawade, H. Yamamoto, Y. Ikeda, V. N. Bhoraskar, and T. Katoh, Nucl. Phys. **A279**, 269 (1977).

¹⁷L. O. Edvardson, L. Westerberg, and G. Ch. Madueme, Nucl. Phys. **A252**, 103 (1975).

- ¹⁸J. V. Maher, J. J. Kolata, and R. W. Miller, *Phys. Rev. C* **6**, 358 (1972).
- ¹⁹A. Buyrn, *Nucl. Data Sheets* **11**, 327 (1974).
- ²⁰F. K. McGowan and W. T. Milner, *Phys. Rev. C* **23**, 1926 (1981).
- ²¹G. Ch. Madueme, *Phys. Rev. C* **24**, 894 (1981).
- ²²T. S. Dumitrescu and I. Hamamoto, *NORDITA Report* 81/49, 1981 (unpublished).
- ²³V. G. Soloviev and N. Yu. Shirikova, *Z. Phys. A* **301**, 263 (1981).
- ²⁴D. R. Bes, P. Federman, E. Maqueda, and A. Zuker, *Nucl. Phys.* **65**, 1 (1965).
- ²⁵P. M. Walker, J. L. S. Carvalho, and F. M. Bernthal, *Phys. Lett.* **116B**, 393 (1982).
- ²⁶A. Bohr and B. R. Mottelson, *Nuclear Structure* (Benjamin, New York, 1975), Vol. II.
- ²⁷D. D. Warner and R. F. Casten, *Phys. Rev. Lett.* **48**, 1385 (1982).
- ²⁸O. Scholten, F. Iachello, and A. Arima, *Ann. Phys. (N.Y.)* **115**, 325 (1978).
- ²⁹K. Neergard and P. Vogel, *Nucl. Phys.* **A145**, 33 (1970).
- ³⁰C. J. Gallagher and V. G. Soloviev, *K. Dan. Vidensk. Selsk. Mat.-Fys. Medd.* **2**, No. 2 (1962).